

MICROSTRIP BAND-REJECT FILTER BASED ON INTER-DIGITAL CAPACITANCE LOADED LOOP RESONATORS

Y. Peng and W. X. Zhang

State Key Lab of Millimeter Waves
Southeast University
Nanjing 210096, China

Abstract—In this paper, the inter-digital capacitance loaded loop resonators (IDCLLRs) are proposed to design microstrip band-reject filters. The analyzed structures are based on the coupling of IDCLLRs to a conventional 50Ω microstrip transmission line. We have firstly studied the frequency response of one-stage IDCLLR-loaded microstrip transmission line. The main features of the IDCLLRs are small dimensions (much smaller than the wavelength at resonance) and more structural parameters (provide flexibility in design); Then a 6-stage IDCLLR-based microstrip band-reject filter was designed and fabricated, it performs relative rejection bandwidth of 8.1% and rejection level of 23 dB. This stop-band is resulted from presence of the artificial medium with negative effective permeability ($\mu_{eff} < 0$). In addition, it is easy to control the rejection bandwidth by only employing different length of inter-digital fingers (for multiple tuning). A 9-stage band-reject filter with multiple tuned IDCLLRs has been fabricated and tested, its relative rejection bandwidth is extended to 11.5%. Simulated and measured results are presented.

1. INTRODUCTION

Recently, a novel family of printed microwave band-pass or band-reject filter has been designed based on the structure of sub-wavelength resonators, started from split ring resonators (SRRs). SRR originally proposed by Pendry consists of a pair of concentric metallic rings with a split etched in opposite sides (Fig. 1(a)) [1]. It has been demonstrated [2] that SRR behaves as LC resonator and can be excited

Corresponding author: Y. Peng (yipeng@seu.edu.cn).

by external time-varying magnetic field with an appreciable component in its axial direction. The resonant frequency of SRR is given by $f_0 = (L_s C_s)^{-1/2}/2\pi$, where L_s and C_s are equivalent inductance and equivalent capacitance of SRR respectively. C_s is the series capacitance of the left- and right-halves of SRR. L_s is the inductance of the ring with approximately average perimeter and width c [3]. The main feature of SRRs are that their size can be made much smaller than its resonant wavelength, thus the periodically arranged SRRs form an equivalent continuous medium with effective permeability μ_{eff} and permittivity ε_{eff} [3]. When a guided wave propagates inside such medium, the effective permeability takes positive/negative values in a narrow band below/above the resonance, and takes extreme values in the vicinity of f_0 . As a result, the propagation is prohibited, the typical stop-band extends not only above f_0 ($\mu_{eff} < 0$), but also in a narrow band below it. These stop-band performances can be applied to planar transmission structure to design band-reject filters. It has been shown that SRR-loaded microstrip line [4–6] and coplanar waveguide (CPW) [7, 8] behave as compact, high Q , band-reject filters with deep stopband in the vicinity of their resonant frequencies.

These characteristics of SRR had been extended to the other sub-wavelength resonators derived from the basic geometry of the SRR, for example, broadside coupled SRR (BC-SRR) [2, 9], spiral resonator (SR) [3], capacitance loaded loop resonator (CLLR) [10, 11], S -ring resonator [12] and complementary split ring resonator (CSRR) [2, 5, 6, 13], etc. But SRRs have less structural parameters. Both L_s and C_s are determined mainly by the dimensions of SRR, but less by its geometry, so it is not sure to obtain desired resonant frequency for a SRR with given dimensions. The other kinds of sub-

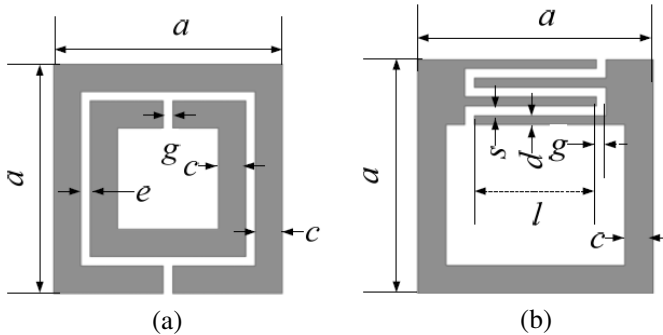


Figure 1. Sub-wavelength resonators. (a) Split ring resonator (SRR). (b) Inter-digital capacitance loaded loop resonator (IDCLLR).

wavelength resonator mentioned above meet the same quandary. In order to hurdle this obstacle, the inter-digital capacitance loaded loop resonators (IDCLLRs) are proposed to construct the band-reject filters in this paper.

The geometry of an IDCLLR is described in Fig. 1(b). Obviously, more structural parameters are provided by the inter-digital structure. A special case of IDCLLR [14] has been used in designing a compact waveguide; In this work, a detail research for frequency response of IDCLLR is performed by both simulation and experiment. A band-reject filter is obtained by a $50\ \Omega$ microstrip line coupling with two arrays of IDCLLRs. A 6-stage IDCLLR-based band-reject filter is fabricated and measured. The rejection bandwidth of the filter can be controlled by employing multiple resonators with slightly different resonant frequencies. The resonant frequencies of IDCLLRs can be tuned easily by only changing inter-digital length l . A 9-stage IDCLLR-based reject-band filter with multiple tuning has been designed and fabricated. The simulated and measured results are presented below for comparison.

2. INTER-DIGITAL CAPACITANCE LOADED LOOP RESONATOR (IDCLLR)

Just like SRRs, the IDCLLRs can be excited by an external magnetic field with polarization along its axis. At resonance, the time-varying magnetic field induces current along the ring, and continues with displacement current throughout the inter-digital capacitance. In general, the inter-digital structure with same width of finger and gap (i.e., $d = s$) corresponds to a maximum capacitance [15]. The quasi-static resonant frequency of IDCLLR is formulated as $\omega_0 = 1/\sqrt{L_0 C_0}$, where L_0 is equivalent inductance of IDCLLR, C_0 is the quasi-static capacitance of the inter-digital capacitor calculated approximately by using [16]

$$C_0(\text{PF}) = \frac{\varepsilon_e 10^{-3} K(k)}{18\pi K'(k)} (N-1)l \quad (1)$$

where ε_e is effective permittivity in microstrip line with strip-width of d , N is the number of fingers, l is the length of each finger; $K(k)$ and $K'(k)$ are complete elliptic function of the first kind and its complementary function, their modulus is $k = \tan^2[d\pi/4(d+s)]$. Obviously, the effective capacitance of IDCLLR depends on so many parameters, resulting in more freedom in designing.

For studying resonant characteristics of IDCLLR, a single cell of IDCLLR-based filter has been designed and fabricated. The geometry

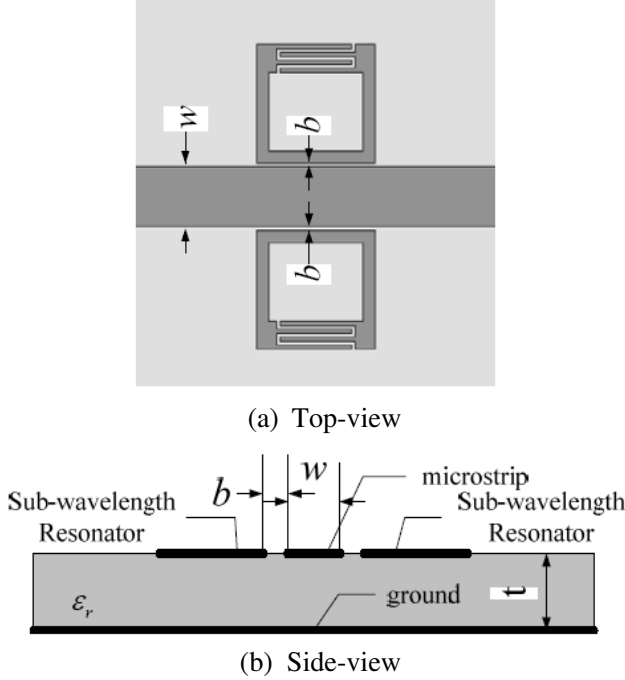


Figure 2. Geometry of IDCLLR-based microstrip one stage band-reject filter.

of the designed filter prototype is shown in Fig. 2. A $50\ \Omega$ microstrip line with strip-width of $w = 3.05\text{ mm}$ and coupled by two IDCLLRs with spacing of $b = 0.2\text{ mm}$ is etched on a Arlon diclad 880 substrate ($\epsilon_r = 2.2$, $t = 1\text{ mm}$). The sizes in the IDCLLR are $a = 6\text{ mm}$, $c = 0.6\text{ mm}$, $g = d = s = 0.2\text{ mm}$, $l = 3.6\text{ mm}$, and the number of fingers is $N = 4$. This filter prototype has been simulated using software HFSS, and measured using Agilent PNA E8363B series vector network analyzer. The results of S_{21} frequency responses described in Fig. 3(a) show the presence of a narrow notch and compare to that of SRR-based filter prototype with sizes of $a = 6\text{ mm}$, $c = 0.6\text{ mm}$, $g = e = 0.2\text{ mm}$ (see Fig. 1(a)). The resonant frequency of IDCLLR is identified by the transmission notch with insertion loss of -12 dB in stop-band, and rejection bandwidth (for -10 dB) of 13 MHz or relative bandwidth 0.39% .

Two kinds of resonators occupy the same area, but the resonant frequency is lower for the IDCLLRs (3.32 GHz) and higher for the SRRs (4.72 GHz). The size in resonant wavelength λ_g of the resonator

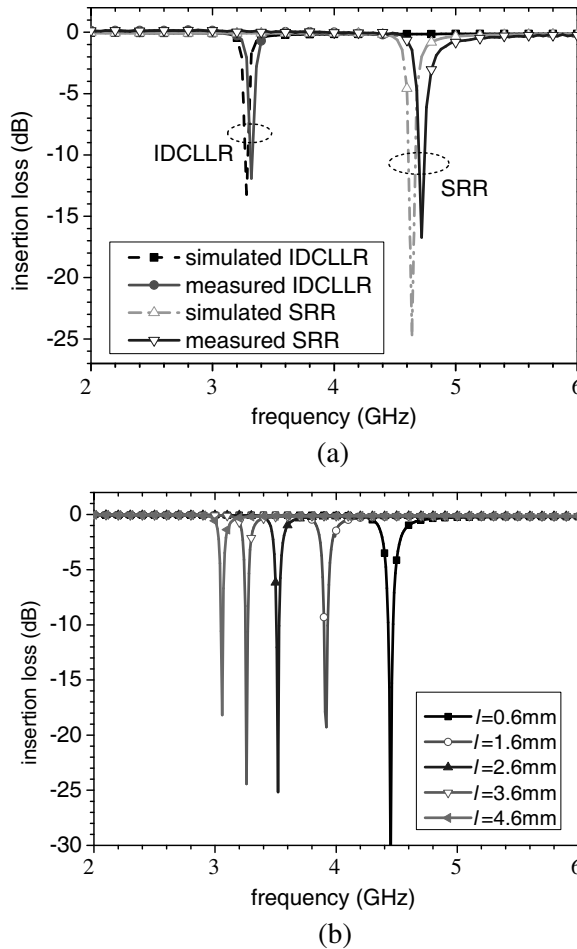
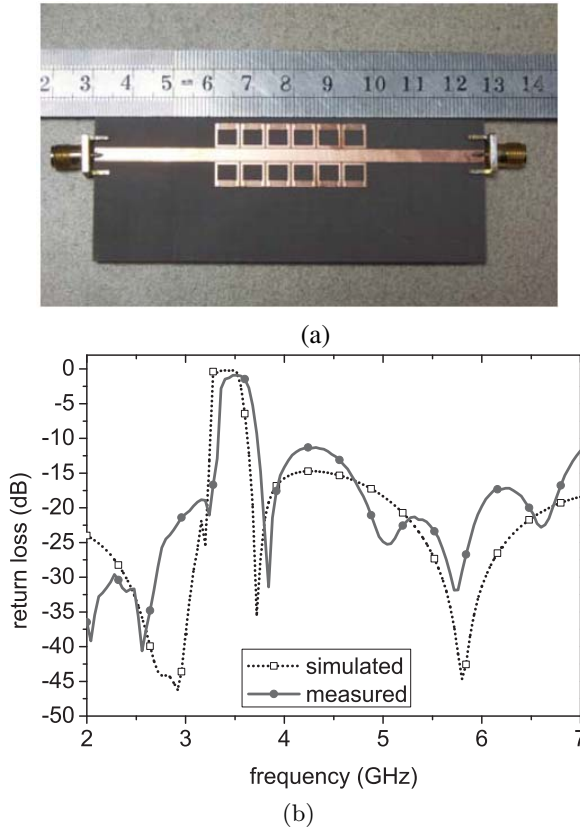


Figure 3. (a) Simulated & measured insertion loss for IDCLLR-based and SRR-based filters. (b) Simulated insertion loss for IDCLLR-based filter with different finger length. *All the cells occupy the same area.

is more compact for the IDCLLRs ($\sim \lambda_g/11$) than the SRRs ($\sim \lambda_g/7$). The resonant frequency of IDCLLRs can be further lower by increasing the number of fingers. So the IDCLLR is more attractive in structure miniaturization. However, since IDCLLRs are a structure of single ring, magnetic coupling between IDCLLRs and line is weaker than that between line and SRRs with double-ring structure. So from Fig. 2(c), we also observe that the maximum insertion loss in the stopband of IDCLLR-based filter is lower than that of SRR-based filter. In order

to improve the properties of stopband of IDCLLR-based filter, it is necessary to increase the number of IDCLLRs stages. A IDCLLR-based multistage filter will be introduced in next section.

Moreover, the resonant frequency of IDCLLR can be adjusted easily by changing parameters of the inter-digital structure. For convenience, we only change the length of finger l and keep s , d , and g (see Fig. 1(b)). From (1), we can expect that the resonant frequency of the structure will be shifted down as increasing the finger length. Fig. 3(b) shows the simulated S_{21} frequency responses of the structure with same area but varied $l = 0.6$ mm, 1.6 mm, 2.6 mm, 3.6 mm, 4.6 mm, respectively. Which result in resonant frequency shift-down within a larger dynamic range from 4.45 GHz (for $l = 0.6$ mm) to 3.08 GHz (for $l = 4.6$ mm), corresponding to a reduction factor of 1.4 times.



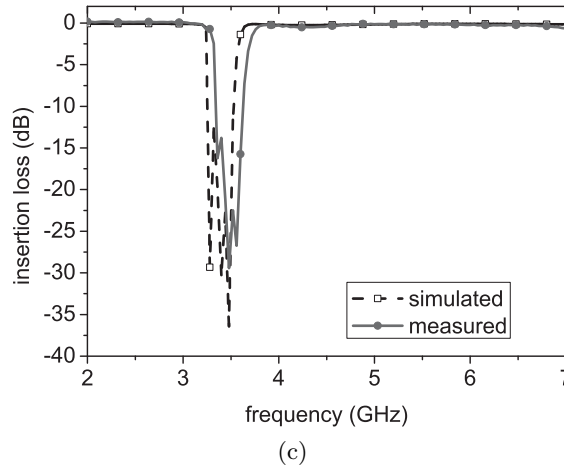


Figure 4. A 6-stage IDCLLR-based band-reject filter. (a) Prototype for testing. (b) Simulated and measured return-loss. (c) Simulated and measured insertion-loss.

3. IDCLLR-BASED BAND-REJECT FILTER DESIGN

The cascade of electrically small IDCLLRs can be considered as a continuous medium with effective constitutional parameters, permeability μ_{eff} and permittivity ε_{eff} , as like that for SRRs. Thus an IDCLLR-based 6-stage band-reject filter has been designed and fabricated as shown in Fig. 4(a). Here the same sizes of six stages IDCLLRs (a total of 12 IDCLLRs) with the spacing of $b = 0.3$ mm are chosen. The structure can be described as one-dimensional medium with μ_{eff} and ε_{eff} . The stopband behavior of the structure can be explained as follow: in a narrow range starting at f_0 , the effective permeability of the structure is negative (i.e., single negative medium (SNG)), and propagating waves become evanescent waves. As a result, the wave propagation is inhibited. Both simulated and measured results of return-loss and insertion-loss are presented in Figs. 4 (b)&(c) respectively. The stop-band (based on rejection level at 10 dB) is observed from 3.34 GHz to 3.62 GHz with 8.1% bandwidth, centered at 3.48 GHz with -23 dB insertion loss. The measured and simulated results are good agreement with minor differences due to possible mismatching in connectors and imperfect fabrication.

For comparing the influence of the number of IDCLLRs on the frequency response of filter, the simulated curves of insertion loss of the filter with different (4, 5, 6, 9) stages are shown in Fig. 5, their stop-band characteristics are listed in Table 1. Obviously, more stages

can enhance the rejection level. However, only the narrow peaked notches can be obtained in the transmission coefficient due to high Q of the IDCLLR resonator, even if employ more IDCLLR pairs. The rejection bandwidth 8.7% of 9-stage filter is only 0.4% enhancement from that 8.3% of 6-stage filter.

The scheme to extend the bandwidth is uneven tuning the multi-stage IDCLLRs into slightly different resonant frequency within the forbidden band [5, 8] by means of different length of inter-digital fingers. A 9-stage prototype is designed and fabricated too as shown in Fig. 6(a). Its fingers length is 3.6 mm for the left three pairs, 3.2 mm for the middle three pairs, and 2.8 mm for the right three pairs of the IDCLLRs. The simulated and measured results of return-loss are shown in Fig. 6(b), the measured stop-band (based on rejection level at 10 dB) is observed from 3.43 GHz to 3.85 GHz with 11.5% bandwidth, centered at 3.64 GHz with -33 dB insertion loss. That is an obvious

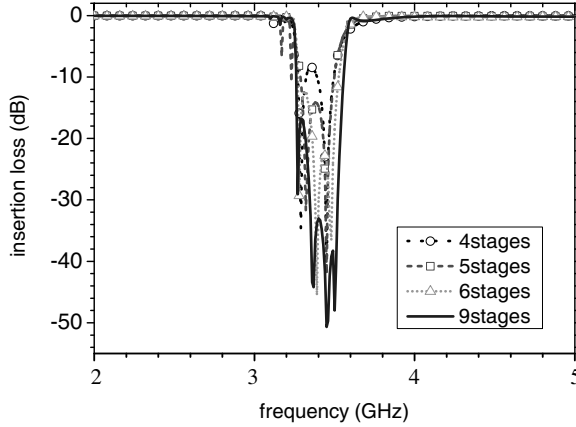


Figure 5. Simulated insertion loss of IDCLLR-based multi-stage filters.

Table 1. Simulated stopband characteristics of IDCLLR-based stopband filter with different number of stages.

Stages	Center frequency	Rejection level	Bandwidth
4	3.386 GHz	8.50 dB	6.7% (-8.5 dB)
5	3.393 GHz	14.4 dB	6.2% (-10 dB)
6	3.388 GHz	23.2 dB	8.3% (-10 dB)
9	3.410 GHz	33.6 dB	8.7% (-10 dB)

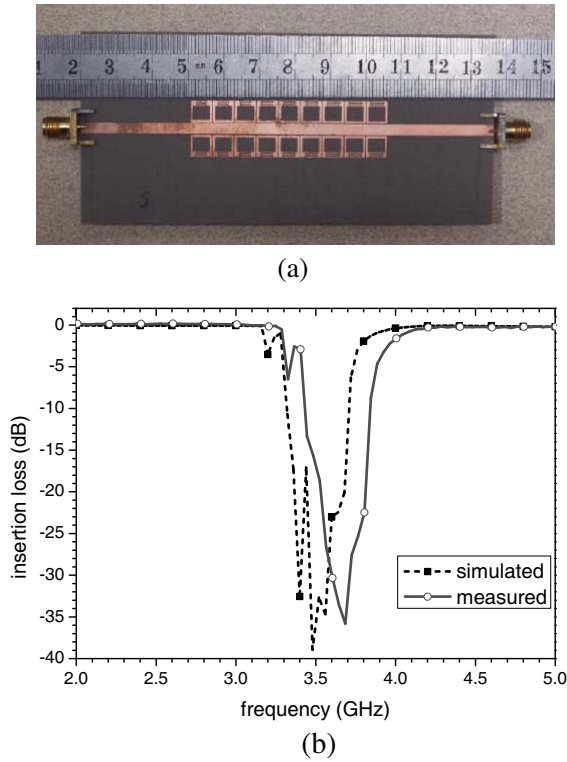


Figure 6. A 9-stage uneven-turning IDCLLR-based band-reject filter. (a) Prototype for testing. (b) Simulated and measured insertion-loss.

improvement, though the stop-band has slight shift from simulated one.

4. CONCLUSION

A comparative analysis of frequency responses of SRR-loaded and IDCLLR-loaded microstrip transmission line have been carried out firstly, the IDCLLRs with the same sizes as SRRs has more compact sizes and larger dynamic range. Secondary, different stages in IDCLLR-loaded filters has been designed, more stages corresponds to more deep rejection level. Furthermore, the uneven-tuning multi-stage IDCLLRs-loaded filter can improve the rejection bandwidth. All designed prototypes have been analyzed by simulation, their computed results have been verified by measurement.

ACKNOWLEDGMENT

This work is supported by National Hightech Project under Grant 2007AA01Z264 of China.

REFERENCES

1. Pendry, J. B., A. J. Holden, D. J. Robbins, and W. J. Stewart, "Magnetism from conductors and enhanced nonlinear phenomena," *IEEE Trans. Microw. Theory Tech.*, Vol. 47, No. 11, 2075–2084, Nov. 1999.
2. Marqués, R., F. Mesa, J. Martel, and F. Medina, "Comparative analysis of edge- and broadside-coupled split ring resonators for metamaterial design — Theory and experiments," *IEEE Transactions on Antennas and Propagation*, Vol. 51, No. 10, 2572–2581, 2003.
3. Baena, J. D., J. Bonache, F. Martín, R. Marqués Sillero, F. Falcone, T. Lopetegi, M. A. G. Laso, J. Garcia-García, I. Gil, M. F. Portillo, and M. Sorolla, "Equivalent-circuit models for split-ring resonators and complementary split-ring resonators coupled to planar transmission lines," *IEEE Trans. Microw. Theory Tech.*, Vol. 53, No. 4, 1451–1461, Apr. 2005.
4. García-García, J., J. Bonache, I. Gil, F. Martín, R. Marqués, F. Falcone, T. Lopetegi, M. A. G. Laso, and M. Sorolla, "Comparison of electromagnetic band gap and split-ring resonator microstrip lines as stop band structures," *Microwave and Optical Tech. Lett.*, Vol. 44, No. 4, 376–379, Feb. 20, 2005.
5. García-García, J., F. Martín, F. Falcone, J. Bonache, J. D. Baena, I. Gil, E. Amat, T. Lopetegi, M. A. G. Laso, M. A. M. Iturmendi, M. Sorolla, and R. Marqués, "Microwave filters with improved stopband based on sub-wavelength resonators," *IEEE Trans. Microw. Theory Tech.*, Vol. 53, No. 6, 1997–2006, Jun. 2005.
6. Öznazı, V. and V. B. Erturk, "A comparative investigation of srr- and csrr-based band reject filters: Simulations, experiments, and discussions," *Microwave and Optical Tech. Lett.*, Vol. 50, No. 2, 519–523, Feb. 2008.
7. Falcone, F., F. Martín, J. Bonache, R. Marqués, and M. Sorolla, "Coplanar waveguide structures loaded with split ring resonators," *Microwave and Optical Tech. Lett.*, Vol. 40, 3–6, Jan. 2004.
8. Martín, F., F. Falcone, J. Bonache, R. Marqués, and M. Sorolla, "Miniaturized coplanar waveguide stopband filters based on

- multiple tuned split ring resonators,” *IEEE Microw. Wireless Compon. Lett.*, Vol. 13, No. 12, 511–513, Dec. 2003.
9. Jelínek, L., J. Macháček, and J. Zehentner, “A magnetic metamaterial composed of randomly oriented SRRs,” *PIERS Online*, Vol. 2, No. 6, 624–627, 2006.
 10. Erentok, A., P. L. Luljak, and R. W. Ziolkowski, “Characterization of a volumetric metamaterial realization of an artificial magnetic conductor for antenna applications,” *IEEE Transactions on Antennas and Propagation*, Vol. 53, No. 1, 160–172, Jan. 2005.
 11. Schurig, D., J. J. Mock, B. J. Justice, S. A. Cummer, J. B. Pendry, A. F. Starr, and D. R. Smith, “Metamaterial electromagnetic cloak at microwave frequencies,” *Science*, Vol. 314, 977–980, Nov. 10, 2006.
 12. Cheng, X. X., H. S. Chen, J. A. Kong, et al., “A bianisotropic left-handed metamaterials compose of *S*-ring resonator,” *PIERS Online*, Vol. 3, No. 3, 241–245, 2007.
 13. Khan, S. N., Q. L. Zhang, and S. He, “Left handed microstrip transmission line loaded with combination of split ring resonator and complementary-SRR,” *Journal of Electromagnetic Waves and Applications*, Vol. 22, No. 13, 1857–1863, 2008.
 14. Xiao, G., J. Mao, and B. Yuan, “An artificial magnetic material with interdigital structure,” *Proc. IEEE AP-S Int. Symp. Dig.*, Vol. 1, 2558–2561, Hawaii, USA, Jun. 10–15, 2007.
 15. Alley, G. D., “Interdigital capacitors and their application to lumped-element microwave integrated circuits,” *IEEE Trans. Microw. Theory Tech.*, Vol. 18, No. 12, 1028–1033, 1970.
 16. Bahl, I. and P. Bhartia, *Microwave Solid State Circuit Design*, 2nd edition, Wiley, New York, 2003.